Comparison between Mercury Intrusion Porosimetry and Nuclear Magnetic Resonance Relaxometry to study the pore size distribution of limestones treated with a new consolidation product

Martina Zuena[1,5], Patrizia Tomasin[2], Maria Francesca Alberghina[3], Anna Longo[3], Maurizio Marrale[3], Salvatore Gallo[4], Elisabetta Zendri[5]

[1] Department of Molecular Science and Nanosystem, Ca' Foscari University of Venice, Via Torino 155, 30170, Venezia Mestre, Italy;
[2] Institute of condensed matter chemistry and technologies for energy, CNR, Corso Stati Uniti 4, 35127 Padova, Italy;
[3] Department of Physics and Chemistry, University of Palermo, Viale delle Scienze, Edificio 18, 90128, Palermo, Italy
[4] Department of Physics, University of Milan, Via Giovanni Celoria 16, 20133, Milan, Italy;
[5] Department of Environmental Sciences, Informatics and Statistics, Ca' Foscari University of Venice, Via Torino 155, 30170, Venezia Mestre, Italy;

Corresponding author: martinazuena@gmail.com; Tel.: +39-3476418021

Abstract
Porosity plays a key factor in the physical and chemical deterioration process of stones. In fact, it controls the dynamics of fluids in stone materials, their movement from the outside to the inside and vice versa, and the different presence of water inside the stones with a consequent control of the durability and resistance to the alteration. Therefore, pore-space properties, such as pore-size distribution and connected porosity, are relevant factors in the evaluation of the efficacy and compatibility of a consolidation treatment. To evaluate these parameters, two different techniques - Mercury Intrusion Porosimetry (MIP) and Nuclear Magnetic Resonance Relaxometry of water ^{1}H nuclei (NMRR) - were adopted in this work to study the performance of a new consolidation product for limestones. This study aims at comparing and combining data obtained by MIP and NMRR. In fact, MIP analysis is a destructive technique which provides quantitative results about the pore structures (pore size distribution and open porosity %). NMRR analysis gives qualitative data and, being both non-destructive and non-invasive, it is possible to obtain the relaxation time distributions (T_2) of water ^{1}H nuclei in the stones' pores before and after the application of a consolidation treatment on the same sample. Furthermore, a correlation between T_2 distribution and pore size distribution has been accomplished and this could provide the NMRR technique with the ability to measure more quantitatively pore size. Experimental results showed that in most cases there is a good correlation between MIP and NMRR data. Therefore, despite NMRR technique is a qualitative analysis, it can be considered a powerful tool to evaluate the change in pore size distribution due to the application of a consolidating agent on stone and, if, as in this case, a calibration with MIP results is performed, the NMRR can provide quantitative information on the pore size distribution.

Keywords: MIP, NMR relaxometry, porosity, stone conservation

1. Introduction

Limestones used in the field of Cultural Heritage are particularly susceptible to a weathering process due to their composition and textural characteristics. In fact, the reaction of carbonate minerals with environmental factors such as air pollution, water, soluble salts and biodeteriogens causes physical and chemical stresses . Open porosity %, the most important aspect in the weathering process, refers to the ratio between the volume of open pores, communicating with each other in a portion of the material, and the total volume.
In order to preserve weathered building materials, calcium ethoxide $Ca(OEt)_2$, a novel product developed during the European collaborative project NANOMATCH , and characterized in previous works , is here subjected to some modifications and applied on three types of limestones as consolidating agent.
When a consolidating treatment is applied to restore the lost material cohesion of a stone, the study of different stones' characteristics, such as pore structure, is relevant to evaluate its performance as consolidating agent. In fact, the physico-mechanical properties of the stone are deeply connected to the pore network which represents the microstructural feature that mostly influences the decay process . Different classifications were developed regarding the description of pore space based on petrogenic aspects, pore geometry or genesis, pore location, pore size and penetration of fluids and gases . Open porosity %, the most important aspect for the weathering process, refers to the ratio between the volume of open holes, communicating with each other in a portion of the material, and the total volume. When a consolidation product is applied on stone, even if it should alter the materials microstructure the lowest possible extent to respect the compatibility criterion , the consolidation effect is usually connected to a small reduction of open porosity, which often simply implies the restoration of the initial porosity of the sound stone.

Several techniques are used to determine the pore structure of porous materials . However, some of them are invasive and destructive. Therefore, when a consolidation product is applied, even if the acquired information is useful, it is not possible to compare data obtained from the same samples before and after the application of the treatment. In this study, the capability of calcium ethoxide to restore the natural porosity of decayed stones (previously aged to simulate weathering materials with a connected variation of their natural open porosity %) is evaluated with two different techniques: Mercury Intrusion Porosimetry (MIP) and Nuclear magnetic resonance relaxometry (NMRR).
MIP is a destructive technique traditionally widely adopted in the field of conservation of building materials , , . Its performance is based on the gradual intrusion of mercury, as a not-wetting liquid, into a porous system when an external pressure is applied .
On the contrary, NMR relaxometry provides data regarding the internal structure of a porous material in a non-invasive and non-destructive way. This technique has been increasingly applied to characterize and monitor works of art in recent years . Thanks to a prior absorption of water under vacuum, which fills the open pores of the stone, it is able to characterize the pore-space structure of high surface-to-volume ratio (S/V) systems. In fact, through the study of the time-evolution of the nuclear magnetization of water ^{1}H nuclei and its return back to the equilibrium condition, after an appropriate sequence of a radiofrequency pulse, it is possible to acquire qualitative information about pore size distribution. The process of the return back to equilibrium is called “relaxation” and it is characterized by a constant decay time named relaxation time. The pore size distributions can be evaluated by analysing relaxation time distribution. In this study, a quantitative calibration of NMR T_2 distributions into a pore size distribution has been achieved by correlating the distributions obtained through MIP and NMRR techniques. Moreover, the combined use of MIP and NMRR allowed to evaluate the performance of the new consolidating treatment to restore the open porosity % of artificially aged samples.

2. Experimental section

2.1. Materials and reagents

Calcium ethoxide, a nanosuspension in a 1:3 solution (v/v) of ethanol and tetrahydrofuran, was produced by ABCR labs (Spain). The initial calcium concentration of this nanosuspension was 46.5 g/L; however, a calcium concentration of 20 g/L showed a good compromise between consolidation effect and aesthetical compatibility, as pointed out during preliminary experiments performed during the NANOMATCH project , . Therefore, to reach a calcium concentration of 20 g/L, the initial product was diluted in three different solvents chosen for their different boiling point and because they are actually used in the restoration field: ethanol, 2-butanol and n-butylacetate. The solvent’s boiling point is an important parameter because it could influence the penetration of the product inside the porous materials . Hence, the studied products based on $Ca(OEt)_2$ are three: $Ca(OEt)_2$ nanosuspension diluted in ethanol (labelled as ETA), $Ca(OEt)_2$ diluted in 2-butanol (labelled as BUT) and $Ca(OEt)_2$ diluted in n-butylacetate (labelled as NBU).
Calcium ethoxide has been compared with CaLoSil E50®, a commercial product based on nanolime, available in the market and employed as stone consolidant. This product is developed by IBZ-Salzchemie (GmbH & Co.KG, Germany) and composed of $Ca(OH)_2$ nanoparticles (50-250 nm) in ethanol with a calcium concentration of 27.05 g/L .To obtain a calcium concentration of 20 g/L - the same established for calcium ethoxide - it was diluted with ethanol. This commercial product is labelled in the text as CAL.
The selection of lithotypes has been restricted to calcareous stones since calcium ethoxide is mainly meant for the consolidation of calcite-based substrates because through the reaction with water and carbon dioxide, it leads to the formation of calcium carbonate, the same component present in limestones. Three different types of limestone were selected:

- Lecce stone (L in the text), a biocalcarenite whose name derives from the city of Lecce (south of Italy), shows a quite homogeneous composition made mainly of calcium carbonate in the form of calcite cement and granules (fragments of fossils of marine organism) together with other minerals such as phosphates, glauconite, quartz and various feldspars .
- Noto stone (N in the text) is a calcarenite with a typical pale cream colour which characterizes the whole architecture of the Noto Valley (Sicily). It is composed of calcium carbonate and several small bioclasts, including foraminifera, echinoids, plankton and bryozoa .
- Vicenza stone (V in the text) is an organogenic limestone extracted near the city of Vicenza and characterized by the presence of micro and macro fragments of foraminifera, bryozoans, algae, and echinoderms . It has a strongly heterogeneous structure and consists of calcium carbonate combined with a small percentage of silicon oxide, aluminium, and iron.

The pore size distribution of stone and the open porosity % values were determined by MIP.
All tests were carried out on quarry stone samples, cut into the right size with a water saw, directly in the quarry: 1x1x4 cm^3 for MIP analysis, where a small part was taken away to perform the analysis (1 mm from the treated surface), and 5x10x2 cm^3 for NMRR analysis. In fact, samples analysed with both techniques cannot be the same because MIP is

destructive while NMRR is non-destructive and allows to analyse the same sample before and after the application of the consolidating treatment.
To work on weathered materials, all the tested stones were previously subjected to a thermal ageing process based on six daily heating-cooling cycles: samples were put in an oven for 6 h at 100°C, cooled to laboratory temperature for 6 h, chilled to -20 ◦C for 6 h and, at the end, warmed to laboratory temperature for 6 h . The thermal ageing process was adopted because thermal cycles can usually cause periodical dimension changes of the building materials exposed to environmental conditions. In fact, being the stone a not good conductor of heat, stress between the surface and the core is originated both in the cooling and in the heating phase of the thermal cycle. Carbonate stones are particularly weathered by this phenomenon because calcite crystals have an anomalous and anisotropic thermal behaviour since upon heating they expand in one direction (usually the main axis) and contract along with others (usually perpendicular to the main axis) at the same time. The effect is a progressive loss of cohesion and an increase in porosity with cleavage of some crystals and detachment the of others , .
The chosen thermal process did not lead to a volumetric or mass change of the samples. Therefore, to evaluate eventual microstructural changes, MIP analysis was performed before and after the ageing process.

2.2. Application procedures and analytical techniques

Two application procedures were used to apply the products on the stones: by brush till saturation (AP1) and by brush with a pre-set number of brush strokes (AP2). Brushing application procedure was chosen because it is the most common practise used in the restoration filed (figure 1).

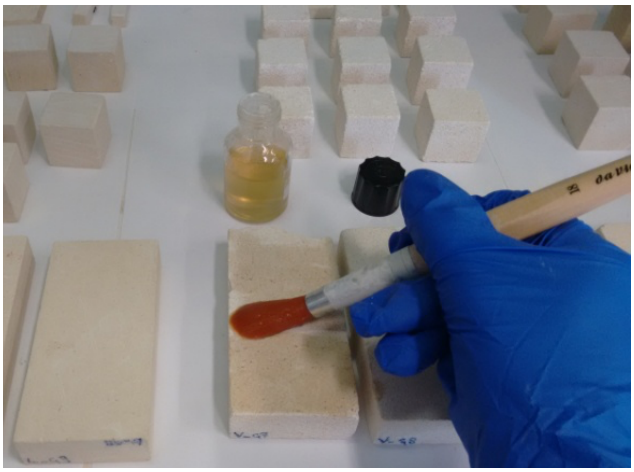

Figure 1. Illustration of the investigated application method: brushing.

AP1 was used for all the products, while AP2 was adopted only for calcium ethoxide diluted in ethanol and CaLoSil E50. For the application AP1, the number of brush strokes was stopped when the surface remained wet for 1 minute. The application AP2 was adopted to avoid a visible colour change of the surface and the number of brush strokes for each stone was decided by preliminary performing a colorimetric measurement after each brush stroke of $Ca(OEt)_2$ diluted in ethanol on stone samples till a value before $\Delta E^* > 5$ was reached. The reference product was applied with the same number of brush strokes. These colorimetric analyses were performed in accordance with the CIEL*a*b* chromaticity diagram and to the NORMAL 43/93 , using a CM2600d Konica Minolta portable spectrophotometer and a spot size of 5 mm diameter. The number of brush strokes used during application procedure AP2 was: 7 for Lecce stone, 8 for Noto stone and 11 for Vicenza stone.
MIP and NMRR analyses were performed one month after the application of the consolidants, to allow a complete carbonation process of the products and the total evaporation of the carrier solvent, based on previous works , . The amount of consolidants remained inside the samples was calculated by weighing the samples before and one month after the application of the products. The values in tab.1 are reported as a mean value of three samples, expressed as kg/m^2, while the associated error is expressed as the standard deviation.

2.2.1. MIP

The pore size distribution was obtained by MIP. The volume of mercury V (mm^3/g) intruded at a given pressure P (kg/cm^2) gives the pore volume value that can be accessed and the resulted open porosity % refers to the volume of open pores present in the stone . The pore-size distribution is determined by the volume of mercury intruded at each pressure increment, whereas the total porosity is determined from the total intruded volume.

The Washburn equation (1), which assumes that pores are cylindrical in shape, explains the relationship between the intrusion pressure and the pore radius size :

$$P = \frac{2\gamma\cos\theta}{r} \quad (1)$$

where P is the intrusion pressure, γ is the mercury surface tension (486.5 mN/m^{-1}), θ is mercury/solid contact angle (141.3°) and r is the pore radius (μm).
MIP analyses were performed on dried samples following NORMAL 4/80 . Results regarding macropores (larger than 50 nm) and mesopores (between 2 and 50 nm) were obtained with Pascal 140 and Pascal 240 Thermo Nicolet instrument (volume resolution 0.001 cc), respectively. To perform this analysis, a small specimen with a maximum weight of 40 mg is taken away from treated and untreated samples (1x1x4 cm^3). Regarding the treated samples, the analysed part corresponds to the first mm from the treated surface, considered as the part most involved in the presence of the consolidants. MIP results are expressed as open porosity % and cumulative volume and with a graphic part which shows: the volume distribution (%) and the pore volume (mm^3/g) in function of the pore radius for each treatment, and a comparison between the pore size distribution among all treated and aged-untreated samples.
For each type of stone, data regarding the open porosity % and the cumulative volume are reported as the average of three analysed samples (both for treated and not treated materials) and the associated error is expressed as standard deviation. Regarding the graphic part, since the three graphs obtained for each analysed sample were comparable, the discussion of the variation of volume distribution % and connected variation of pores dimension is related to one of them.

2.2.2. NMRR

NMRR measurements were carried out on prismatic samples (10x5x2 cm^3) by a relaxometer mq-ProFiler equipped with a single-sided magnet (Bruker Biospin ®, Italy) which works at a Larmor frequency of about 15 MHz. The sensitive volume xyz from which the resonant conditions were obtained is about 2x0,2x0,8 cm^3, where the x and y axes are parallel and perpendicular to the magnet surface, respectively; while, z coincides to the direction of the main magnetic field and to the distance analysed by the treated surface. In this case, the analysed depth is 2 mm. The pore types were obtained by analysing the number and peak position of T_2 spectrum . Transverse relaxation decays were obtained by performing the Carr-Purcell-Meiboom-Gill (CPMG) pulse sequence . In this sequence, the echo time to 44 μs was set and the total number of echo was chosen equal to 8000. After each sequence, a recycle delay of 2 ms was set to allow the longitudinal magnetization to fully recover before the next pulse sequence. Experimental data, acquired through the Minispec software, were turned into T_2 distributions by the inversion of the relaxation decay data using the UPEN algorithm .
In order to correlate the relaxation time distribution with the pore size distribution, we followed the procedure described in Gao et al. .

In particular, it was exploited that transverse relaxation time is approximately related to pore size according to the following equation (2):

$$\frac{1}{T_2} = \frac{1}{T_{2S}} = \rho_2 \frac{S}{V} \quad (2)$$

where T_{2S} is the surface relaxation time, ms; ρ_2 is the surface relaxivity, μs/m; S is the surface area, μm^2; V is the pore volume, μm^3; S/V is the specific surface area of pores (1/μm). Actually, the relationship between T_2 and the pore size distribution is a power function because of the complexity of the pore structure. It can be shown that (3):

$$r_t = CT_2^{1/n} \quad (3)$$

where r_t is a pore throat radius which is supposed to be proportional to the pore body radius, C is a constant and 1/n is the power exponent .
In order to obtain a pore size distribution from the NMR relaxometry measurements, the logarithm of both member of the previous equation was calculated obtaining the expression (4) and both MIP and NMR distributions were interpolated and shifted in order to maximize the match between these distributions:

$$\ln r_t = \ln C + \frac{1}{n}\ln T_2 \quad (4)$$

Then, the r_t values of MIP were plotted against T_2 values from NMR relaxometry and the C and 1/n values were obtained through a best fitting procedure . All the T_2 distributions reconstructed for the analysed samples report also the pore size obtained via this calibration with MIP data.
NMRR analyses were performed on samples previously dried in an oven and afterwards located in a box where vacuum was created. Then, they were saturated with distilled water. Before the analysis, the saturated samples were completely covered with a plastic film in order to avoid any leak or evaporation of water during the ten-minute measurement. All the analyses were carried out at room temperature and the same set of samples was analysed before and after the application of treatments.

3. Results and discussion

3.1. Lecce stone

The characterization of sound Lecce stone in terms of pore size distribution and open porosity % is obtained with MIP analysis. This stone shows a pore size distribution between 0.1-2 μm and an open porosity % of 34.4 ± 0.5 (Figure S1 in supplementary materials).
The ageing process lead to an increase in both total open porosity % and cumulative volume (Table 1). The dry matter retained after one month is also reported in Table 1.

Table 1. Lecce stone samples: amount of dry matter retained after one month from the applications evaluated for samples analysed with both MIP and NMRR and porosity data obtained by MIP.

Sample	Dry matter retained MIP (Kg/m^2)	Dry matter retained NMRR (Kg/m^2)	Total open porosity (%)	Cumulative volume (mm^3/g)
L_NA*	-	-	34.4 ± 0.5	201.8 ± 2.1
L_NT**	-	-	37.6 ± 0.9	223.8 ± 1.3
L_ETA_AP1	0.016 ± 0.011	0.026 ± 0.002	34.1 ± 0.6	190.3 ± 4.4
L_NBU_AP1	0.012 ± 0.003	0.016 ± 0.003	34.7 ± 0.7	216.5 ± 7.2
L_BUT_AP1	0.018 ± 0.007	0.017 ± 0.006	34.2 ± 0.3	205.5 ± 5.3
L_CAL_AP1	0.063 ± 0.008	0.047 ± 0.005	36.8 ± 0.6	216.7 ± 3.2
L_ETA_AP2	0.025 ± 0.001	0.023 ± 0.005	34.5 ± 0.9	201.6 ± 1.8
L_CAL_AP2	0.022 ± 0.006	0.014 ± 0.003	34.1 ± 0.3	211.3 ± 3.4

*NA: unaged and untreated stone, **NT: aged and untreated stone

Starting with the results obtained with AP1, all the products based on $Ca(OEt)_2$ bring to a decrease in both total open porosity and cumulative volume distribution to the natural value of the sound stone (34.4 % ± 0.5). A different result is obtained with CaLoSiL which is not effective. However, despite CAL is the product mostly retained inside the stone, its low reduction of porosity respect to the treatments based on $Ca(OEt)_2$ could be related to a layer formed by this product on the stone's surface rather than a good penetration inside the sample.
Looking in more detail the changes in pore radius distribution, samples treated with ETA (Fig. 2b) show a small reduction of volume distribution % for pores with a radius between 1-4 μm and a small increase in volume distribution % for pores of smaller dimension (0.1-0.8 μm) respect to untreated stone (Fig. 2a). In samples treated with NBU (Fig. 2c) and CAL (Fig. 2e) a decrease in volume distribution % for pores with a radius between 1-4 μm respect to untreated stone is observed, with a higher decrease for NBU. Furthermore, an increase in volume distribution % for pores with a radius between 0.1- 1 μm is registered. Finally, even if samples treated with BUT present a reduction of open porosity %, it causes only a visible decrease in volume distribution % for pores between 2-4 μm and a modest increase in small pores (<0.1 μm) (Fig. 2d).
Figure 2f reports a comparison of pores size distribution curves between treated and untreated samples. It shows that especially NBU causes a change of pore radius distribution respect to untreated stone. All the products seem to distribute in particular into the bigger pores (>1 μm), reducing their volume distribution % and consequently increasing the volume distribution % of pores with a radius between 0.1- 1 μm. Instead, BUT seems to remain only into the pores with a radius between 2-4 μm.

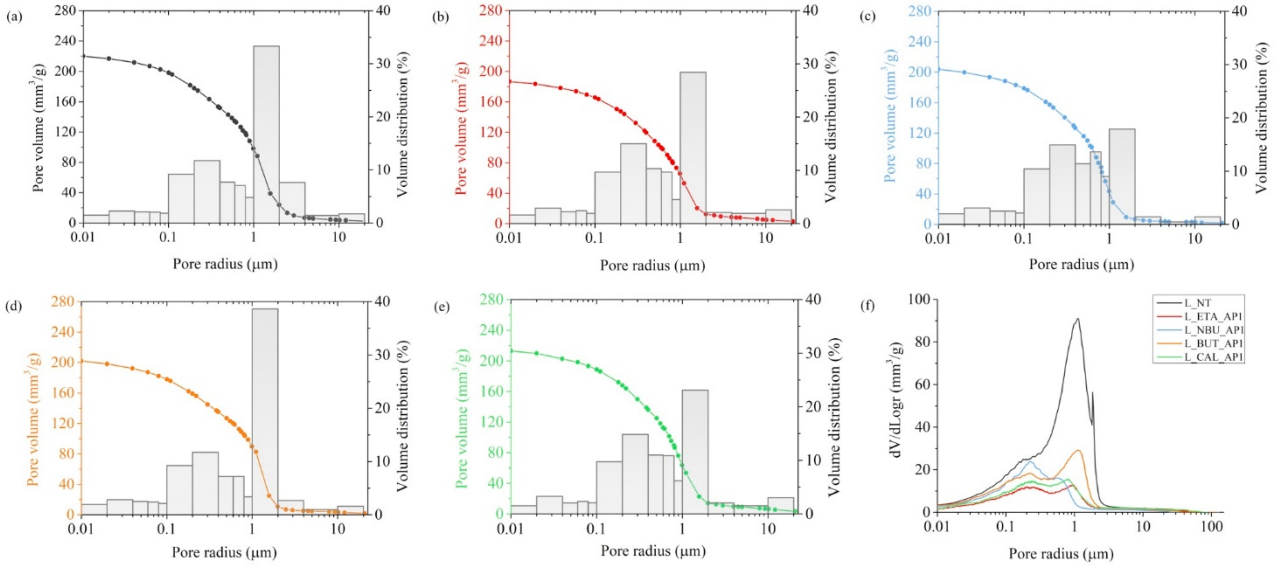

Figure 2. MIP results for Lecce treated with AP1: cumulative pore volume and volume distribution versus pore radius of (a) L_NT, (b) L_ETA_AP1, (c) L_NBU_AP1, (d) L_BUT_AP1 and (e) L_CAL_AP1; (f) pore size distribution curves expressed as log differential intruded volume (mm^3/g) versus pore radius (µm) reported for all treated and aged-untreated samples (NT).

Changes in pores size distribution due to the treatments applied with AP1 procedure obtained through NMRR analysis are evaluated through transverse relaxation time distributions (T_2). For this samples, the dry matter retained after one month from the application is reported in Table 1.

The results (Fig. 3) agree with MIP measurements. In fact, all treatments show a visible variation for pores of larger dimension (T_2> 10 ms which corresponds to about 1 µm) and a small variation for pores of lower dimensions (T_2< 10 ms).

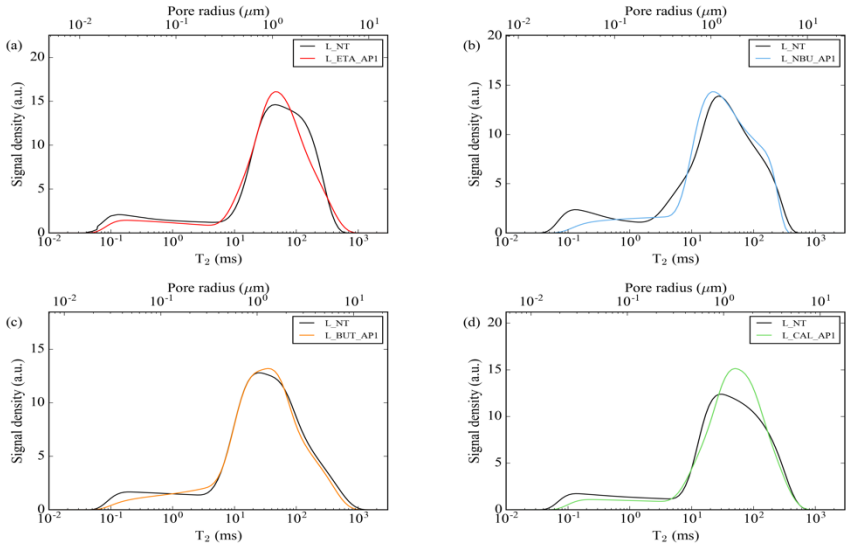

Figure 3. Comparison of T_2 distribution functions before and after treatment with application AP1:(a) L_ETA_AP1, (b) L_NBU_AP1, (c) L_BUT_AP1 and (d) L_CAL_AP1. NT: aged-untreated stone

With the application procedure AP2, MIP results (Table 1) show how both treatments lead to a porosity value similar to natural stone (34.4 % ± 0.5). However, samples treated with CAL show a pore radius distribution more similar to untreated support respect to those treated with ETA (Fig. 4c). In fact, while ETA reduces the volume distribution % of pores with radius between 1-4 µm, leading to an increase in volume distribution % of pores of smaller dimensions (< 1µm) (Fig. 4a), CAL reduces only the volume distribution % of pores with radius between 2-4 µm (Fig. 4b).

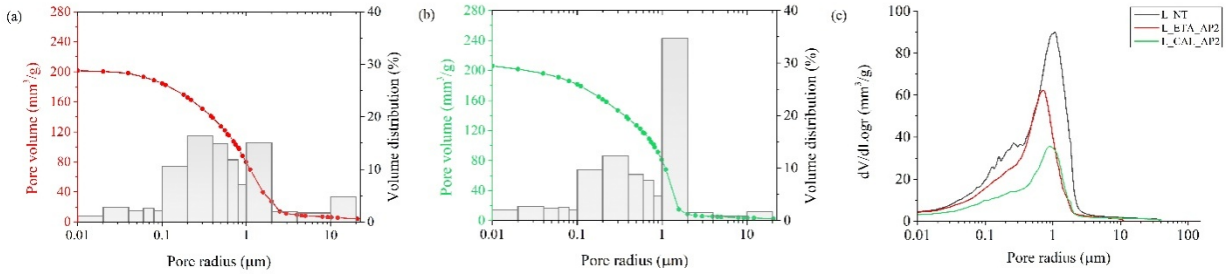

Figure 4. MIP results for Lecce treated with AP2: cumulative pore volume and volume distribution versus pore radius of (a) L_ETA_AP2 and (b) L_CAL_AP2; (c) pore size distribution curves expressed as log differential intruded volume (mm^3/g) versus pore radius (μm) reported for all treated and aged-untreated samples (NT).

Moving to NMRR results, the quantity of dry matter retained after one month from the application is reported in Table 1.

Both treatments (Fig. 5) cause a variation of pore size distribution for pores of larger dimensions (T_2 >10 ms), respect to untreated stone. For pores of lower dimension (T_2 <10 ms which corresponds to about 1μm) a higher change is obtained with ETA (Fig. 5a), while CAL maintains a pore distribution more similar to untreated stone (Fig. 5b), as showed also for MIP measurements (Fig 4).

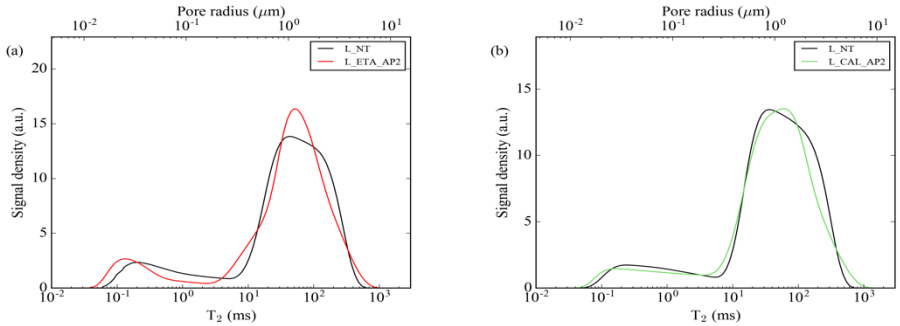

Figure 5. Comparison of T_2 distribution functions before and after treatment, application AP2: (a) L_ETA_AP2 and (b) L_CAL_AP2. NT: aged-untreated stone.

In conclusion, there is a good correlation between MIP and NMRR data also for application procedure AP2. In fact, L_ETA presents a variation of pores of both dimensions, bigger and smaller as showed for MIP results (Fig. 4a). Instead, L_CAL maintains a pore size distribution more similar to untreated stone and shows a variation only for pores of bigger dimensions as observed for MIP. Therefore, NMRR can provide clear information to understand for which type of pores, the treatments cause a variation in the pore size distribution.

3.2. Noto stone

MIP results obtained from unaged stone shows a pores size distribution between 1-4 μm and an open porosity % value of 30.3 ± 0.9 (figure S2 in supplementary materials).

The ageing process led to an increase in total open porosity % and cumulative volume respect to unaged stone (Table 2).

MIP results concerning AP1 shows that all the products based on calcium ethoxide and the reference one are successful in reducing the total open porosity % of the stone leading to a porosity value similar to unaged stone (Table 2).

Table 2. Noto stone samples: amount of dry matter retained after one month from the applications evaluated for samples analysed with both MIP and NMRR and porosity data obtained by MIP.

Sample	Dry matter retained MIP (Kg/m^2)	Dry matter retained NMRR (Kg/m^2)	Total open porosity (%)	Cumulative volume (mm^3/g)
N_NA*	-	-	30.3 ± 0.9	155.9 ± 2.4
N_NT**	-	-	34.5 ± 2.6	172.1 ± 0.9
N_ETA_AP1	0.208 ± 0.005	0.028 ± 0.003	29.6 ± 0.2	156.1 ± 3.1
N_NBU_AP1	0.020 ± 0.013	0.010 ± 0.001	29.6 ± 0.6	166.7 ± 2.7
N_BUT_AP1	0.019 ± 0.008	0.020 ± 0.005	29.6 ± 0.6	154.1 ± 15.1

N_CAL_AP1	0.047 ± 0.013	0.057 ± 0.013	29.2 ± 0.8	153.3 ± 4.9
N_ETA_AP2	0.033 ± 0.002	0.031 ± 0.003	30.1 ± 1.9	172.1 ± 0.9
N_CAL_AP2	0.025 ± 0.001	0.019 ± 0.003	28.9 ± 0.8	166.3 ± 5.6

*NA: unaged and untreated stone, **NT: aged and untreated stone.

Figure 6 shows pore size distribution curves, cumulative pore volume and volume distribution for each product. All treatments lead to a very small increase in volume distribution % of pores with a radius between 0.1 and 1 µm. Instead, for pores greater than 1 µm, the situation is different depending on the product. In fact, N_ETA and N_CAL present a high decrease in volume distribution % of pores between 2-4 µm and an increase in volume distribution % of pores between 1-2 µm (Fig. 6b and 6e, respectively) respect to untreated stone (Fig. 6a); instead, N_NBU and N_BUT show a different effect with a small increase in volume distribution % of pores between 1-2 µm and a small decrease in volume distribution % for those ones between 2-4 µm (Fig.6c and 6d, respectively). In fact, looking at figure 6f, a change in the pore size distribution was visible for all products with respect to untreated stone. This variation is particularly evident for pore radius larger than 1µm.

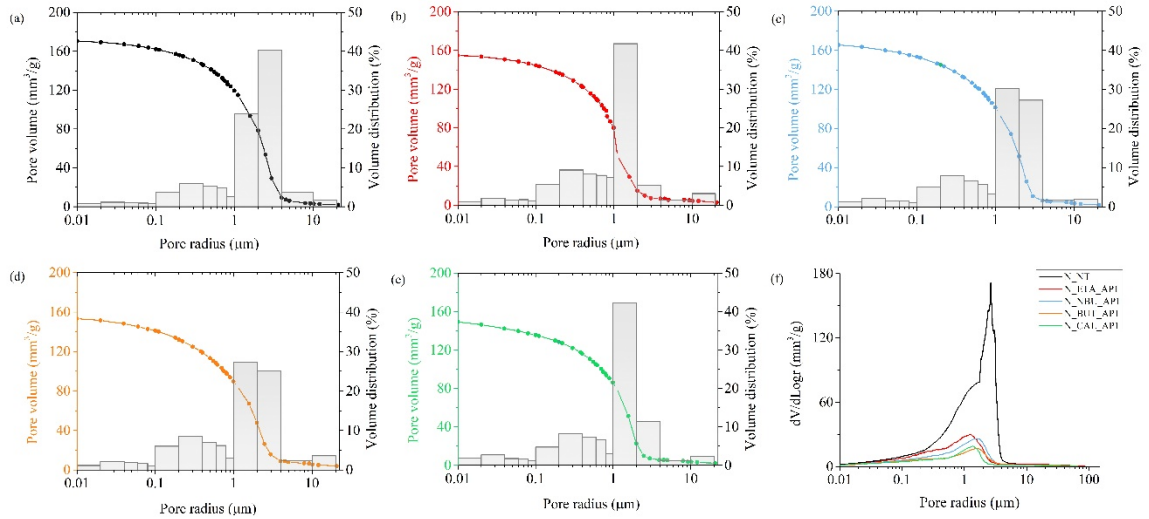

Figure 6. MIP results for Noto stone treated with AP1: cumulative pore volume and volume distribution versus pore radius of (a) N_NT, (b) N_ETA_AP1, (c) N_NBU_AP1, (d) N_BUT_AP1 and (e) N_CAL_AP1; (f) pore size distribution curves expressed as log differential intruded volume (mm^3/g) versus pore radius (µm) reported for all treated and aged-untreated samples (NT).

Dry matter retained after one month for samples analysed with NMRR is listed in Table 2. T_2 distribution functions show a variation for pores of bigger dimension (T_2>10 ms), for all treatments (Fig. 7). This results agree with MIP data which showed a volume distribution modification in pores of bigger dimensions for all treatments. The part of the curve related to pores of smaller dimension (T_2< 10 ms) does not show evident change for samples treated with ETA and BUT. Instead, a variation is showed for N_NBU and N_CAL. These results partly agree with MIP, for which a variation of volume distribution % for pores of smaller dimension is slightly evident for all treatments.

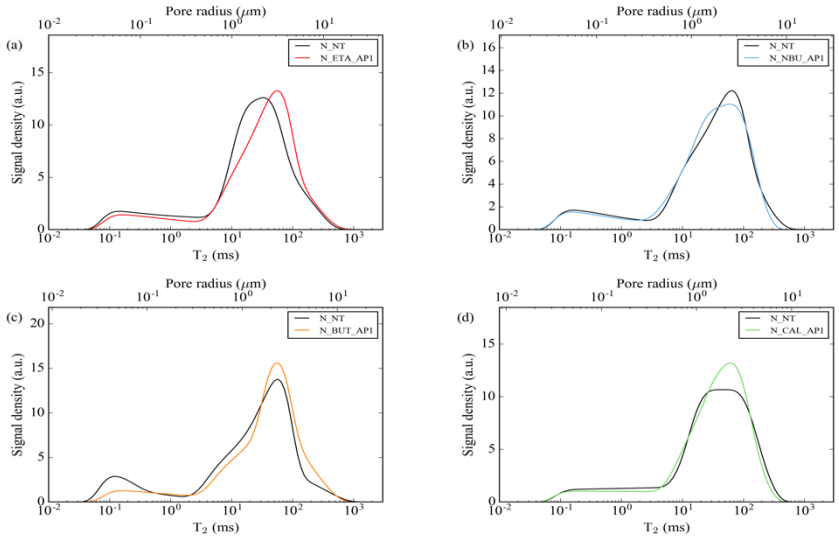

Figure 7. Comparison of T_2 distribution functions before and after treatment, application AP1: (a) N_ETA_AP1, (b) N_NBU_AP1, (c) N_BUT_AP1 and (d) N_CAL_AP1. NT: aged-untreated stone.

Changes in total open porosity % and cumulative volume due to the treatments applied with AP2 are shown in Table 2. The results indicated that both treatments lead to a reduction of porosity value similar to unaged sample (30.3 ± 0.9 %). All products lead to a small increase in pores of smaller dimensions (0.01 – 1 μm), with a higher change for ETA respect to CAL. Furthermore, ETA shows a decrease in volume distribution % of pores with a radius between 2-10 μm and an increase in volume distribution % of pores with a radius between 1-2 μm (Fig. 8a). Instead, N_CAL shows a small decrease in volume distribution % of pores with a radius between 1-4 μm and a bit increase in volume distribution % of pores with a radius greater than 4 μm (Fig. 8b). By observing a comparison between all samples (Fig. 8c) both treatments show a variation of the maximum of the curve, moving it to smaller dimensions of pores.

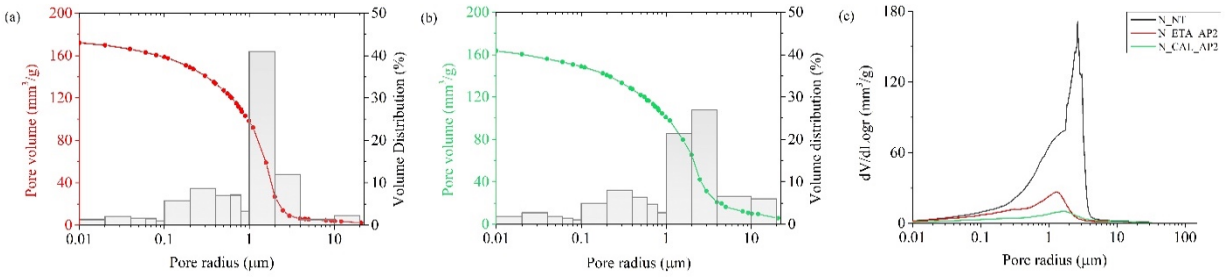

Figure 8. MIP results for Noto stone treated with AP1: cumulative pore volume and volume distribution versus pore radius of (a) N_ETA_AP2 and (b) N_CAL_AP2; (c) pore size distribution curves expressed as log differential intruded volume (mm^3/g) versus pore radius (μm)reported for all treated and aged-untreated samples (NT).

The quantity of dry matter retained after one month for samples analysed with NMRR is reported in Table 2. T_2 distribution functions of treated samples are different with respect to untreated ones for both applied products (Fig. 9). In particular, bigger changes are visible for pores of larger dimensions (T_2> 10 ms), as detected with MIP. Instead for pores of lower dimensions an evident change is visible mostly for N_ETA, while the curves related to N_NT and N_CAL are quite similar.

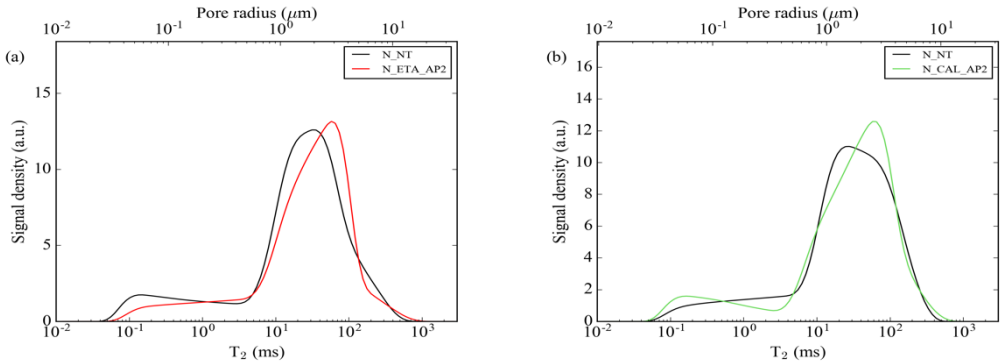

Figure 9. Comparison of T_2 distribution functions between treated and untreated samples, application AP2: (a) N_ETA_AP2 and (b) N_CAL_AP2. NT: aged-untreated stone

The overall results obtained for Noto stone show that all treatments, including the reference one, are able to reduce the total open porosity % of samples to a value similar to the sound stone. For both application procedures, there is a good correlation between the variation of pore size dimension detected with MIP and NMRR. Also in this case NMRR is helpful in understanding a variation in pore size dimensions due to the consolidation treatments.

3.3. **Vicenza stone**

Vicenza unaged stone presents a bimodal pore size distribution between 0.1-0.4 and 1-11 μm and an open porosity of 31.2 % ± 1.9 (figure S3 in supplementary materials).
For this type of stone, the ageing process led to a decrease in total open porosity % and in cumulative volume (Table 3). Probably, this reduction may be related to an internal stress induced by the ageing process, which led to the clogging of internal open porosity.
Starting from the application AP1, CAL maintains a value of total open porosity % similar to untreated stone. Instead, treatments based on calcium ethoxide reduce this parameter in an excessively way.

Table 3. Vicenza stone samples: amount of dry matter retained after one month from the applications evaluated for samples analysed with both MIP and NMRR and porosity data obtained by MIP.

Sample	Dry matter retained MIP (Kg/m^2)	Dry matter retained NMRR (Kg/m^2)	Total open porosity (%)	Cumulative volume (mm^3/g)
V_NA*	-	-	31.2 ± 1.9	149.9 ± 12.7
V_NT**	-	-	28.3 ± 0.8	131.5 ± 4.1
V_ETA_AP1	0.039 ± 0.001	0.014 ± 0.003	24.9 ± 0.4	113.1 ± 4.2
V_NBU_AP1	0.076 ± 0.004	0.034 ± 0.002	24.4 ± 0.9	149.0 ± 2.2
V_BUT_AP1	0.040 ± 0.005	0.028 ± 0.002	24.5 ± 1.1	123.8 ± 3.8
V_CAL_AP1	0.038 ± 0.030	0.113 ± 0.025	28.1 ± 1.4	139.8 ± 3.2
V_ETA_AP2	0.053 ± 0.006	0.035 ± 0.003	24.5 ± 1.1	121.9 ± 10.4
V_CAL_AP2	0.062 ± 0.001	0.022 ± 0.003	24.1 ± 1.2	130.3 ± 1.6

*NA: unaged and untreated stone, **NT: aged and untreated stone.

Respect to untreated samples (Fig. 10a), ETA causes a small reduction of volume distribution % of pores with radius between 2-4 μm and also a variation for pores of smaller dimension (0.01-1 μm) (Fig. 10b). NBU leads to a decrease in volume distribution % of pores with a radius between 0.1-0.4 μm and 2-10 μm and an increase in those ones between 0.4- 1 μm (Fig. 10c). BUT reduces the volume distribution % of pores with radius between 0.1-0.2 μm and greater than 10 μm but increases those ones between 0.2-1 μm and 1-10 μm (Fig. 10d). Finally, CAL leads to a decrease in volume distribution % of pores between 0.1-0.2 μm, 2-4 μm and higher than 10 μm and it leads to an increase in volume distribution % of pores between 0.2-0.4 μm and 4-10 μm (Fig. 10e). Therefore, even if CAL leads to a change in pore size distribution of treated stone, it maintains a value of open porosity % similar to untreated/aged stone. Figure 10f shows how every treatment causes a pore size distribution variation by preserved at the same time a bimodal distribution.

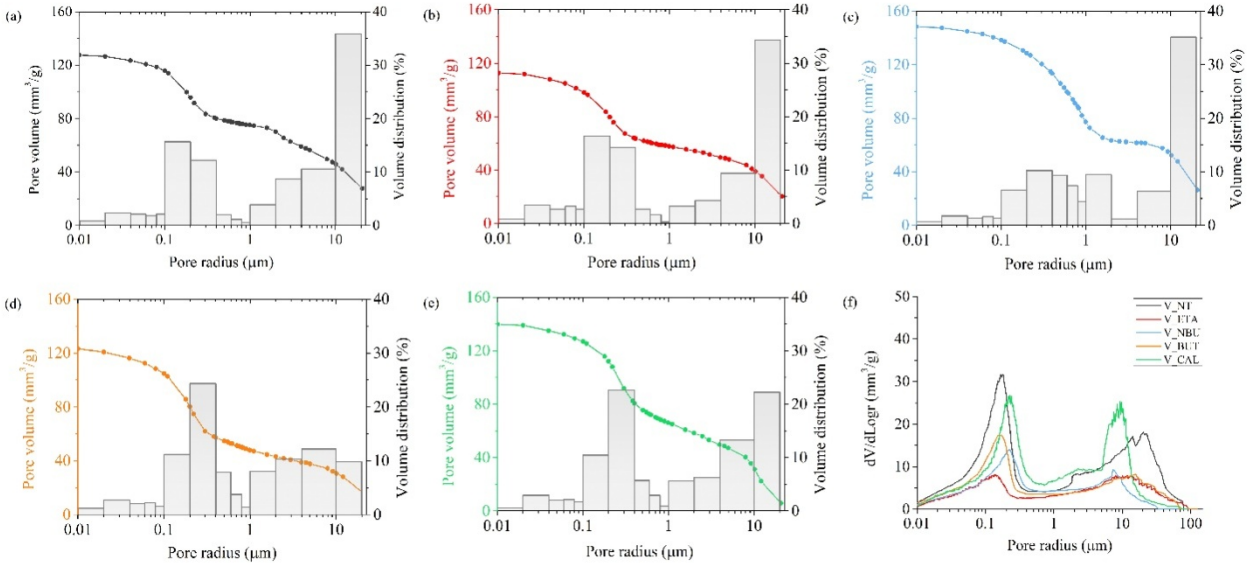

Figure 10. MIP results for Vicenza stone treated with AP1: cumulative pore volume and volume distribution versus pore radius of (a) V_NT, (b) V_ETA_AP1, (c) V_NBU_AP1, (d) V_BUT_AP1 and (e) V_CAL_AP1; (f) pore size distribution curves expressed as log differential intruded volume (mm^3/g) versus pore radius (μm) reported for all treated and aged-untreated samples (NT).

For the application procedures AP1, the quantity of dry matter retained after one month for samples analysed with NMRR is reported in Table 3.

The analysis of T_2 distribution functions shows that ETA (Fig. 11a) causes a change especially for pores of smaller dimensions and in a lower way for pores of bigger dimensions. NBU (Fig. 11b) leads to a change in both pore dimensions, as detected also by MIP (Fig. 10c). Finally, both BUT (Fig. 11c), and CAL (Fig. 11d) show a variation of both pores of smaller and bigger dimension, in accordance with MIP results (Fig. 10d and 10e, respectively).

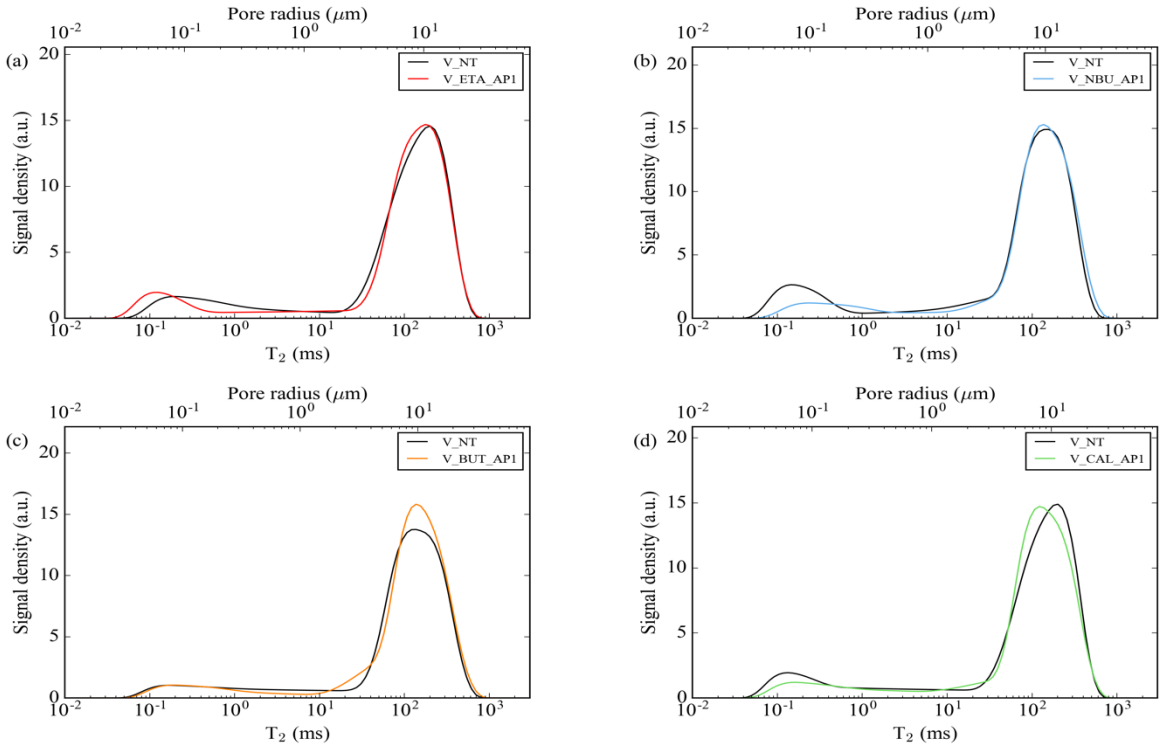

Figure 11. Comparison of T_2 distribution functions before and after treatment on Vicenza stone, application AP1: (a)

V_ETA_AP1, (b) V_NBU_AP1, (c) V_BUT_AP1 and (d) V_CAL_AP1. NT: aged-untreated stone

Changes in total open porosity %, cumulative volume obtained by MIP and retained product due to application procedure AP2 are reported in Table 3. In detail, ETA leads to a higher reduction of volume distribution % of pores with radius >10 µm and a small increase of those ones between 4-10 µm and < 0.1 µm (Fig.12a); CAL reduces the volume distribution % of pores with radius > 2 µm and slightly increased those ones with a radius between 0.2-0.4 µm and 1 µm (Fig. 12b). Also with this type of application procedure, both treatments maintain a bimodal pore radius distribution as shown in figure 12c.

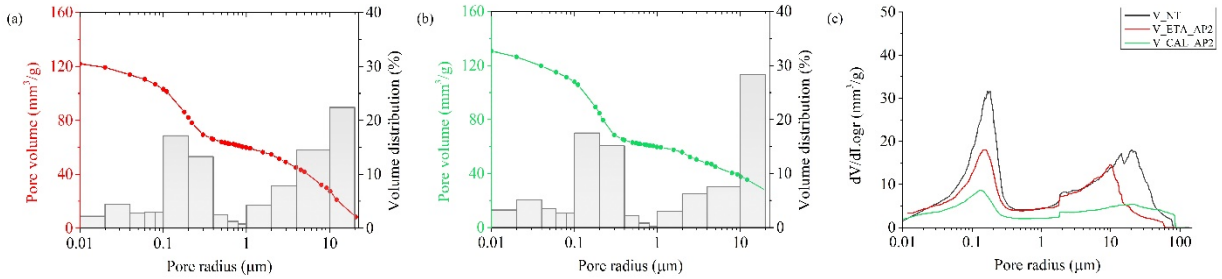

Figure 12. MIP results for Noto stone treated with AP2: cumulative pore volume and volume distribution versus pore radius of (a) V_ETA_AP2 and (b) V_CAL_AP2; (f) pore size distribution curves expressed as log differential intruded volume (mm^3/g) versus pore radius (µm) reported for all treated and aged-untreated samples (NT).

The quantity of dry matter retained after one month in samples treated with AP2 and analysed with NMRR is reported in Table3. In both cases, NMRR results agree with MIP data. In fact, V_ETA shows a visible change in T_2 curves before and after treatment for pores of bigger dimension and also a variation for pores of smaller dimensions (Fig. 13a). V_CAL presents a modification of the curve for both pores of smaller (T_2< 10 ms) and larger dimension (T_2>10 ms) (Fig. 13b).

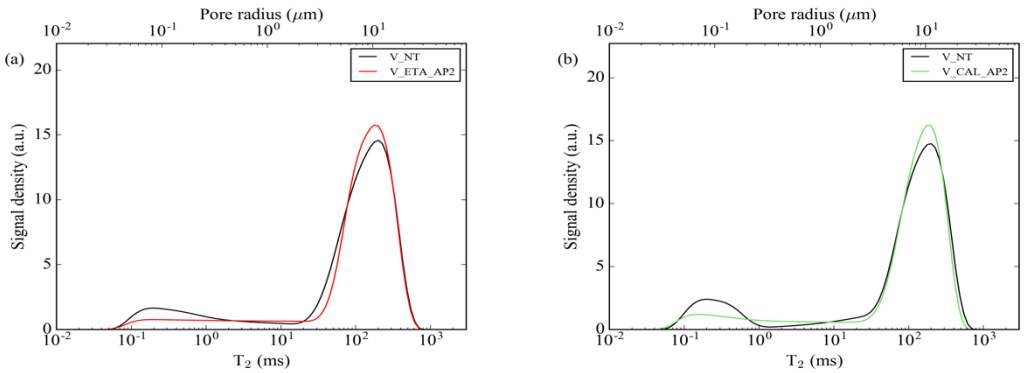

Figure 13. Comparison of T_2 distribution functions before and after treatment on Vicenza stone with application AP2:(a) V_ETA_AP2 and (b) V_CAL_AP2. NT: aged-untreated stone.

For Vicenza stone, a good correlation between MIP and NMRR is observed. In fact, as showed by MIP, both application AP1 and AP2 produce a change in pore size distribution well correlated with the variation of T_2 distribution functions.

Conclusion

Three different consolidating treatments based on calcium ethoxide have been applied to three limestones frequently used in the field of Cultural Heritage. Changes in pore-size distribution due to the application of consolidants were evaluated with two different techniques: mercury intrusion porosimetry and nuclear magnetic resonance relaxometry. Through a calibration between MIP and NMRR measurements, NMR relaxometry allowed to quantitatively get information on pore size and to investigate in a non-destructive way the change in pore-size distributions due to the application of these consolidating agents by making an observation of the same sample before and after treatment, differently from MIP technique, which is quantitative but destructive.

The overall results showed that, in most cases, there is a good correlation between the quantitative results obtained by MIP and the ones observed with NMRR. In fact, variation in the pore size distribution between untreated and treated samples evidenced with MIP is often correlated with the change of the shape of T_2 distribution obtained with NMRR.
By considering the consolidation effect, all products based on calcium ethoxide were able to restore the initial total open porosity % of unaged samples for Lecce stone and Noto stone; therefore, the consolidant maintained a good compromise between consolidation action and alteration of natural properties of the stones. A different result was obtained for Vicenza stone: in fact, the reference product maintained a value of open porosity % similar to the aged samples (which in this case was lower respect to unaged stone) while all products based on calcium ethoxide led to a decrease in open porosity % respect to aged samples. In general, no evident correlation was observed between the quantity of retained dry matter and the consolidation effect.
.
Conflict of interest: The authors declare that they have no conflict of interest.

A**cknowledgments**

The NANOMATCH Project (Nano-systems for the conservation of immovable and moveable polymaterial Cultural Heritage in a changing environment) has received funding from the European Union's Seventh Program for research, technological development and demonstration under grant agreement No. [283182]. Dr. Dorothy Fontana and Luigi Tranchina are kindly acknowledged for their valuable support provided during the NMRR analysis.

Data availability: the raw/processed data required to reproduce these findings cannot be shared at this time as the data also forms part of an ongoing study.

References

[2] D. Camuffo, Physical weathering of stones, Sci. Total Environ. 167 (1995) 1–14. doi:https://doi.org/10.1016/0048-9697(95)04565-I.

[3] A.E. Charola, Salts in the deterioration of porous materials: an overview, JAIC. 39 (2000) 327–343. doi:https://doi.org/10.1179/019713600806113176.

[4] D. Pinna, Coping with Biological Growth on Stone Heritage Objects: Methods, Products, Applications, and Perspectives, Apple Academic Press, 2017.

[5] I. Natali, P. Tomasin, F. Becherini, A. Bernardi, C. Ciantelli, M. Favaro, O. Favoni, V.J.F. Pérez, I.D. Olteanu, M. Dolores, R. Sanchez, A. Vivarelli, A. Bonazza, Innovative consolidating products for stone materials: field exposure tests as a valid approach for assessing durability, Herit. Sci. 3 (2015) 1–13. doi:10.1186/s40494-015-0036-3.

[6] E. Bourguignon, P. Tomasin, V. Detalle, J. Vallet, M. Labouré, I. Olteanu, M.A. Chiurato, A. Bernardi, F. Becherini, Calcium alkoxides as alternative consolidants for wall paintings: Evaluation of their performance in laboratory and on site, on model and original samples, in comparison to conventional products, J. Cult. Herit. 29 (2017) 54–66. doi:https://doi.org/10.1016/j.culher.2017.07.008.

[7] M. Zuena, P. Tomasin, D. Costa, J. Delgado-Rodrigues, E. Zendri, Study of Calcium Ethoxide as a New Product for Conservation of Historical Limestone, Coating. 8 (2018) 103. doi:10.3390/coatings8030103.

[8] M. Zuena, E. Zendri, D. Costa, J. Delgado-Rodrigues, N. El Habra, P. Tomasin, Calcium Ethoxide as Consolidant for Porous Limestones: Influence of the Solvent, Coatings. 9 (2019) 83. doi:10.3390/coatings9020083.

[9] R. Fort, S. Ordo, D. Benavente, Durability estimation of porous building stones from pore structure and strength, 74 (2004) 113–127. doi:10.1016/j.enggeo.2004.03.005.

[10] C. Di Benedetto, P. Cappelletti, M. Favaro, S.F. Graziano, A. Langella, D. Calcaterra, A. Colella, Porosity as key factor in the durability of two historical building stones : Neapolitan Yellow Tuff and Vicenza Stone, Eng. Geol. 193 (2015) 310–319. doi:10.1016/j.enggeo.2015.05.006.

[11] S. Snethlage, R. Siegesmund, Stone in Architecture: Properties, Durability, 4th editio, 2011. doi:10.1007/978-3-642-14475-2.

[12] P. Maravelaki-Kalaitzaki, N. Kallithrakas-Kontos, D. Korakaki, Z. Agioutantis, S. Maurigiannakis, Evaluation of silicon-based strengthening agents on porous limestones, Prog. Org. Coatings. 57 (2006) 140–148. doi:10.1016/j.porgcoat.2006.08.007.

[13] J. Delgado Rodrigues, A. Grossi, Indicators and ratings for the compatibility assessment of conservation actions, J. Cult. Herit. 8 (2007) 32–43. doi:10.1016/j.culher.2006.04.007.

[14] Italian Recommendation NORMAL 20/85, Conservazione dei materiali lapidei: Manutenzione ordinaria e straordinaria, Ist. Cent. Del Restauro (ICR), Rome. (1985).

[15] V. Cnudde, A. Cwirzen, B. Masschaele, P.J.S. Jacobs, Porosity and microstructure characterization of building stones and concretes, Eng. Geol. 103 (2009) 76–83. doi:10.1016/j.enggeo.2008.06.014.

[16] A.T. Watson, C.T.P. Chang, Characterizing porous media with NMR methods, Prog. Nucl. Magn. Reson. Spectrosc. 31 (1997) 343–386. doi:https://doi.org/10.1016/S0079-6565(97)00053-8.

[17] L.M. Anovitz, D.R. Cole, Characterization and Analysis of Porosity and Pore Structures, Rev. Mineral. Geochemistry. 80 (2015) 61–164. doi:http://dx.doi.org/10.2138/rmg.2015.80.04.

[18] J.V. Brakel, S. Modry, M. Svata, Mercury porosimetry: state of the art, Powder Technol. 29 (1981) 1–12. doi:https://doi.org/10.1016/0032-5910(81)85001-2.

[19] M.J. Mosquera, T. Rivas, B. Prieto, B. Silva, Microstructural changes in granitic rocks due to consolidation treatments: their effects on moisture transport, in: Proc. Og 9th Int. Congr. Deterior. Conserv. Stone, 2000: pp. 601–607. doi:https://doi.org/10.1016/B978-044450517-0/50146-X.

[20] G. Taglieri, J. Otero, V. Daniele, G. Gioia, L. Macera, V. Starinieri, A. Elena, The biocalcarenite stone of Agrigento (Italy): Preliminary investigations of compatible nanolime treatments, J. Cult. Herit. 30 (2018) 92–99. doi:10.1016/j.culher.2017.11.003.

[21] J.L.P. Bernal, M.A. Bello, Fractal geometry and mercury porosimetry Comparison and application of proposed models on building stones, Appl. Surf. Sci. 185 (2001) 99–107. doi:https://doi.org/10.1016/S0169-4332(01)00649-3.

[22] L. Appolonia, G.C. Borgia, V. Bortolotti, R.J.S. Brown, P. Fantazzini, G. Rezzaro, Effects of hydrophobic treatments of stone on pore water studied by continuous distribution analysis of NMR relaxation times, 19 (2001) 509–512.

[23] R. Viola, A. Tucci, G. Timellini, P. Fantazzini, NMR techniques: A non-destructive analysis to follow microstructural changes induced in ceramics, J. Eur. Ceram. Soc. 26 (2006) 3343–3349. doi:10.1016/j.jeurceramsoc.2005.09.055.

[24] N. Proietti, D. Capitani, V. Di Tullio, Applications of Nuclear Magnetic Resonance Sensors to Cultural Heritage, Sensors. 14 (2014) 6977–6997. doi:10.3390/s140406977.

[25] C. Nunes, L. Pel, J. Kunecky, Z. Slízková, The influence of the pore structure on the moisture transport in lime plaster-brick systems as studied by NMR, Constr. Build. Mater. 142 (2017) 395–409. doi:https://doi.org/10.1016/j.conbuildmat.2017.03.086.

[26] M. Brai, C. Casieri, F. De Luca, P. Fantazzini, M. Gombia, C. Terenzi, Validity of NMR pore-size analysis of cultural heritage ancient building materials containing magnetic impurities, Solid State Nucl. Magn. Reson. 32 (2007) 129–135. doi:10.1016/j.ssnmr.2007.10.005.

[27] M. Brai, M. Camaiti, C. Casieri, F. De Luca, P. Fantazzini, Nuclear magnetic resonance for cultural heritage, Magn. Reson. Imaging. 25 (2007) 461–465. doi:10.1016/j.mri.2006.11.007.

[28] X. Li, Y. Kang, M. Haghighi, Investigation of pore size distributions of coals with different structures by nuclear magnetic resonance (NMR) and mercury intrusion porosimetry (MIP), Measurement. 116 (2018) 122–

128. doi:10.1016/j.measurement.2017.10.059.

[29] G. Borsoi, B. Lubelli, R. van Hees, R. Veiga, A.S. Silva, L. Colla, L. Fedele, P. Tomasin, Effect of solvent on nanolime transport within limestone: How to improve in-depth deposition, Colloids Surfaces A Physicochem. Eng. Asp. 497 (2016) 171–181. doi:https://doi.org/10.1016/j.colsurfa.2016.03.007.

[30] CaLoSiL®. Colloidal nano-particles of lime for stone and plaster consolidation. Technical Leaflet. IBZ-Salzchemie GmbH & Co. KG.: Halsbrücke, Germany. Available online: https://ibz-freiberg.de/downloads/pdf/produkte/tm/eng/CaLoSiL_E_IP_NP.pdf, n.d. https://ibz-freiberg.de/downloads/pdf/produkte/tm/eng/CaLoSiL_E_IP_NP.pdf.

[31] D. D'Agostino, Moisture dynamics in an historical masonry structure: The Cathedral of Lecce (South Italy), Build. Environ. 63 (2013) 122–133. doi:https://doi.org/10.1016/j.buildenv.2013.02.008.

[32] M.F. La Russa, G. Barone, C.M. Belfiore, P. Mazzoleni, A. Pezzino, Application of protective products to Noto calcarenite (south-eastern Sicily): a case study for the conservation of stone materials, Env. Earth Sci. 62 (2011) 1263–1272. doi:10.1007/s12665-010-0614-3.

[33] S. Scrivano, L. Gaggero, J.G. Aguilar, Porosity characterization of fresh and altered stones by ultrasound velocity and mercury intrusion porosimetry, Geophys. Res. Abstr. 18 (2016) 9418.

[34] J. Rodríguez Gordillo, M.P. Sáez Pérez, Comportamiento físico del mármol blanco de Macael (España) por oscilación térmica de bajo y medio rango Performance of Spanish white Macael marble exposed to narrow- and medium-range temperature cycling, Mater. Construcción. 60 (2010) 127–141. doi:10.3989/mc.2010.44107.

[35] G. Torraca, Lectures on Materials Science for Architectural Conservation, The getty conservation institute, Los Angeles, 2009.

[36] E. Franzoni, E. Sassoni, G.W. Scherer, S. Naidu, Artificial weathering of stone by heating, J. Cult. Herit. 14 (2013) e85–e93. doi:10.1016/j.culher.2012.11.026.

[37] NORMAL 43/93 Misure colorimetriche di superfici opache (Italian normative on stone material- colorimetric measurement of opaque surfaces). Commissione Beni Culturali UNI NORMAL, 1993.

[38] NORMAL 4/80 Distribuzione del volume dei pori in funzione del loro diametro (italian normative on stone material- Distribution of pores volume vs their diameter). Commissione Beni Culturali UNI NORMAL, 1980.

[39] C. Volzone, N. Zagorodny, Applied Clay Science Mercury intrusion porosimetry (MIP) study of archaeological pottery from Hualfin Valley, Catamarca, Argentina, Appl. Clay Sci. 91–92 (2014) 12–15. doi:http://dx.doi.org/10.1016/j.clay.2014.02.002.

[40] E.W. Washburn, The Dynamics of Capillary Flow, Phys. Rev. 17 (1921) 273–283. doi:https://doi.org/10.1103/PhysRev.17.273.

[41] J. Rouquerol, D. Anvir, C.W. Fairbridge, D.H. Everett, J.H. Haynes, N. Pernicone, J.D.F. Ramsay, K.S.W. Sing, K.K. Unger, Recommendations for the characterization of porous solids, Pure Appl. Chem. 66 (1994) 1739–1758.

[42] H.Y. Carr, E.M. Purcell, Effects of diffusion on free precession in nuclear magnetic resonance experiments, PH YSI CAI Rev. 94 (1954).

[43] G.C. Borgia, R.J.S. Brown, P. Fantazzini, Uniform-penalty inversion of multiexponential decay data, 132 (1998) 65–77. papers3://publication/uuid/B434929D-4E80-4CCB-BC9A-4A0F208F2E94.

[44] F. Gao, Y. Song, Z. Li, F. Xiong, L. Chen, X. Zhang, Z. Chen, J. Moortgat, Quantitative characterization of pore connectivity using NMR and MIP: A case study of the Wangyinpu and Guanyintang shales in the Xiuwu basin, Southern China, Int. J. Coal Geol. 197 (2018) 53–65. doi:10.1016/j.coal.2018.07.007.